Carbon – Science and Technology

ISSN 0974 – 0546

http://www.applied-science-innovations.com

ARTICLE Received : 17/07/2013, Accepted : 14/11/2013

Special Section on Advanced (Non-Carbon) Materials

Magnetic properties of monodispersed α-Fe_2O_3 nanoparticles synthesized via a chemical precursor

Mahesh Patange [(#)], Jeevan Jadhav [(#)], and Somnath Biswas [(*)]

The LNM Institute of Information Technology, Jaipur-302031, Rajasthan, India.

[#] Contributed equally; * Corresponding Author, Tel: +91-7597171575; Fax: +91-141-2689014/5189214.

We report a novel sol-gel type chemical synthesis technique to develop monodispersed magnetic hematite (α-Fe_2O_3) nanoparticles. The obtained α-Fe_2O_3 nanoparticles have an average size of ~23 nm with a hexagonal crystal structure (space group R$\bar{3}$c) of lattice parameters a = 0.5034 nm and c = 1.374 nm. The samples were characterized with X-ray diffraction (XRD), scanning electron microscope (SEM), high resolution-transmission electron microscope (HRTEM) and vibrating sample magnetometer (VSM).

Keywords : α-Fe_2O_3, sol-gel method, XRD and VSM.

Introduction : Magnetic iron oxide nanoparticles attract much attention of researchers due to its wide range of potential applications including magnetic fluids, gas sensors, catalysis, biomedicine/biotechnology, magnetic resonance imaging (MRI) and data storage **[1-5].** Thermodynamically, hematite (α- Fe_2O_3) is the most stable in the family of iron (III) oxides : α- Fe_2O_3, β-Fe_2O_3, maghemite (γ-Fe_2O_3), and ε-Fe_2O_3. The *d-d* transitions and legend to metal charge transfer play important roles in tuning the *n*-type semiconducting band gap of hematite. Hematite shows interesting properties like high photochemical stability, low-toxicity and suitable redox potential for photo catalytic water dissociation. Visible light response and photochemical stability makes it apposite for use in solar cells and to eliminate organic pollutant in water. However, the short hole diffusion length, high rate of electron-hole recombination, and limited penetration depth are the major drawbacks for performance optimization **[6-9]**. Various morphological structures in α-Fe_2O_3 have been studied, *e.g.*, shuttle-like, plate-shaped nanocrystals, ring shaped, wires of α- Fe_2O_3, rod-like and flower-like α- Fe_2O_3 **[10, 11]**. For the synthesis of α- Fe_2O_3 nanoparticles, the well studied methods are chemical co-precipitation, hydrothermal, solvothermal, ball milling, forced hydrolysis, micro-emulsion technique and sol-gel method **[10, 11]**.

Here, we report a novel synthesis technique of α-Fe_2O_3 nanoparticles via a sol-gel type chemical process involving a reaction between an aqueous solution of Fe^{3+} ions and a homogeneous aqueous solution of *poly*-vinyl alcohol (PVA) and sucrose.

Materials and Methods :

Materials : Analytical grade ferric nitrate [$Fe(NO_3)_2.9H_2O$] was purchased from Merck. PVA (mol. wt. 1,50,000, degree of polymerization ~1800) and sucrose were purchased from Fisher

Scientific and were employed as-received without any further treatment.

Methods :

1. Synthesis of iron oxide nanoparticles : 100 ml of 0.02 M aqueous ferric (III) nitrate nonahydrate was mixed homogeneously with 25 % ammonia (5 ml) in an aqueous solution of 4.0 % PVA and 40.0 % sucrose with constant stirring at 55 - 60°C. In this reaction, pH was maintained at 9 - 10. A black colored gel was formed after 24 h of aging at room temperature after the reaction. Slow heating of the gel at 70 - 80°C in a water bath gives a dried fluffy precursor mass. Fine grain powders of re-crystallized α-Fe_2O_3 particles were obtained by heating the grinded precursor at 400 - 600°C for 1h in ambient air. This process was previously reported by S. Biswas *et al.* for the synthesis of stable CrO_2 nanoparticles at low temperature [12].

2. Physical Characterization :

2.1 XRD analysis : XRD analysis of the samples was carried out using a Panalytical`s X`Pert Pro model X-ray diffractometer with CuKα radiation.

2.2 Microstructural analysis : The microstructure in the derived samples was analyzed with SEM (JEOL JSM-6036) and HRTEM (JEOL JEM-2100).

2.3 VSM analysis : Magnetic hysteresis loop (M-H curve) of the hematite particles were recorded at room temperature using a Lake Shore VSM with a maximum field of 15 k Oe.

Results and Discussion :

1. XRD Analysis : Figure (1) shows the XRD pattern of the derived powders after heating the dried precursor at 500 °C for 1 h in air. Another sample heated at 400 °C for 1 h shows an X-ray amorphous nature, which is due to the presence of a thick layer of residual carbon over the hematite particles.

The sample obtained by heating the precursor at 500°C for 1 h shows eleven prominent peaks. The observed pattern fits well with JCPDS card no. 33 - 664 with lattice parameter values of a = 0.5034 nm and c = 1.374 nm, which confirms the formation of α-Fe_2O_3 phase [13]. The peaks reveal the high crystallinity in the synthesized hematite nanoparticles. Average crystallite size calculated from the peak widths using Debye-Scherrer formula is ~23 nm. Table (1) shows the detail of the Rietveld analysis.

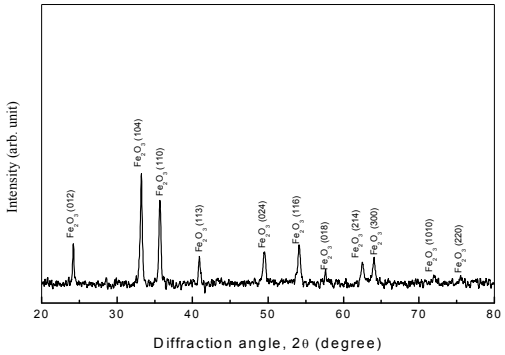

Figure (1) : X-ray diffraction in derived α-Fe_2O_3 powders after heating the precursor at 500°C for 1h in ambient air.

Table (1) : XRD data of α-Fe_2O_3 powders heated at 500°C

Diffraction angle 2θ (º)	Observed d_{hkl} value (nm)	Calculated d_{hkl} value (nm)	Calculated crystallite size (nm)
24.21	0.3684	0.3680	24.55
33.21	0.2700	0.2698	26.44
35.68	0.2519	0.2516	25.46
40.90	0.2207	0.2205	25.00
49.52	0.1864	0.1840	20.83
54.11	0.1694	0.1693	22.91
57.62	0.1599	0.1599	35.25
62.49	0.1485	0.1485	19.64
64.08	0.1453	0.1453	21.82
71.97	0.1315	0.1310	15.80
75.43	0.1259	0.1258	7.55

2. SEM and HRTEM Analyses : Figure (2a) displays the SEM image of the derived samples

after heating the precursor at 500 °C for 1 h. Monodispersed particles of α-Fe_2O_3 with a narrow size distribution can be observed in the micrograph. Figure (2b) shows an HRTEM image of the same samples with finer details. As can be observed, the hematite particles have distorted spherical shapes. The observed widths of ~ 25 nm in the particles match well with the estimated crystallite size from XRD analysis.

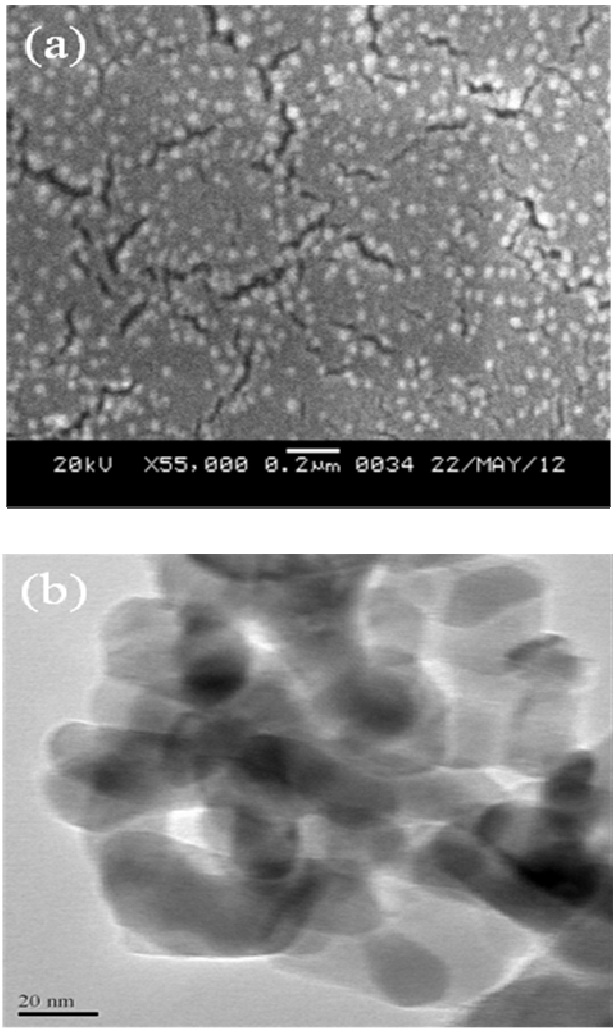

Figure (2) : (a) SEM and (b) HRTEM images of α-Fe_2O_3 nanoparticles calcined at 500°C for 1 h.

3. VSM Analysis : Figure (3) shows the M-H hysteresis loop in the samples calcined at 500°C for 1 h. The observed values of saturation magnetization, remanent magnetization, and coercivity are 2.59 emu/g, 0.19 emu/g, and 37.80 Oe, respectively. The saturation and remanent magnetization values observed in these samples are lower than reported values in similar samples.

Morin transition takes place in hematite at T_M ~260 K; below and above T_M it shows anti-ferromagnetic and ferromagnetic nature, respectively. Below T_M, spins were oriented along the trigonal (111) *c* axis and act as antiferromagnetic uniaxially. Spins associate with basal plane above the T_M were perpendicular to (111) *c* axis, so magnetic moment compensates each other, as a result weak ferromagnetism is introduced **[14]**. As the particle size decreases, transition takes place from multi-domain to a single domain system. The saturation and remanent magnetization decreases with decreasing particle size. On the other hand, coercivity increases because it reaches a maximum value at the critical size for single domain.

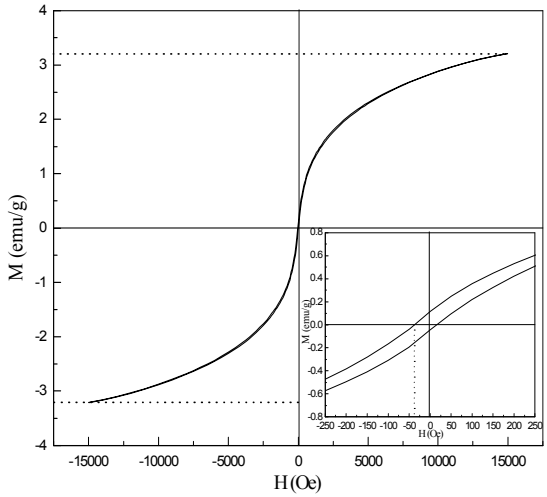

Figure (3) : Room-temperature M-H curve in the derived samples after heating the precursor at 500°C for 1 h in ambient air.

Conclusions : α-Fe_2O_3 nanoparticles have been successfully synthesized by a novel technique via a polymer precursor. In an aqueous solution of PVA, -OH groups have a stereo regularity through which PVA forms micelles. Micellar form of PVA act as a surfactant and adsorb Fe^{3+} ions, forming a metal ion-polymer precursor. The prepared α-Fe_2O_3 nanoparticles are well dispersed in nature without agglomeration. SEM and HRTEM were used to investigate the microstructure in the samples and magnetic properties of the samples was studied at room temperature using a VSM.

Acknowledgments : The authors sincerely thank (i) Sophisticated Analytical Instrument Facility (SAIF), Panjab University, Chandigarh, (ii) North-Eastern Hill University (NEHU), Shillong, and (iii) Indian Institute of Technology, Kanpur for providing us the instrumental facilities.

References :

[1] A. H. Lu, E. L. Salabas, F. Schuth, Magnetic nanoparticles: synthesis, protection, functionalization and application, Angew. Chem. Int. Ed., 46(8) (2007) 1222 - 1244.

[2] X. Wu, Y. Guo, L. Wan, C. Hu, α-Fe_2O_3 nanostructures: inorganic salt-controlled synthesis and their electrochemical performance toward lithium storage, J. Phys. Chem. C 112(43) (2008) 16824 - 16829.

[3] A. G. Nasibulin, S. Rackauskas, H. Jiang, Y. Tian, P. Reddy Mudimela, S. D. Shandakov, L. I. Nasibulina, J. Saini, E. I. Kauppuinen, Simple and rapid synthesis of α-Fe_2O_3 nanowires under ambient conditions, Nano. Res. 2(5) (2009) 373 - 379.

[4] Z. Guo, D. Zhang, S. Wei, Z. Wang, A. B. Karki, Y. Li, P. Bernazzani, D. P. Young, J. A. Gomes, D. L. Cocke, T. C. Ho, Effects of iron oxide nanoparticles on polyvinyl alcohol: interfacial layer and bulk nanocomposites thin film, J. Nanopart. Res. 12(7) (2010) 2415 - 2426.

[5] Y. Wang, Z. Zhu, F. Xu, X. Wei, One-pot reaction to synthesize superparamagnetic iron oxide nanoparticles by adding phenol as reducing agent and stabilizer, J. Nanopart. Res. 14(4) (2012) 755 - 761.

[6] S. Yarahmadi, A. A. Tahir, B. Vaidhyanathan, K. G. U. Waijayantha, Fabrication of nanostructured electrodes using ferrocene for solar hydrogen generation, Mater. Lett. 63(5) (2009) 523 - 526.

[7] T. K. Townsend, E. M. Sabio, N. D. Browning, F. E. Osterloh, Photocatalytic water oxidation with suspended alpha-Fe_2O_3 particles effects of nanoscaling, Energy Environ. Sci. 4(10) (2011) 4270 - 4275.

[8] M. Nakao, T. Hamaguchi, M. Furubayshi, K. Nagato, Patterning of α-Fe_2O_3 nanowires by pressing a microstructured mold and their field-emission properties, Microelectron. Eng. 88(8) (2011) 2697 - 2699.

[9] B. Y. Yu, S. Y. Kwak, Carbon quantum dots embedded with mesoporus hematite nanospheres as efficient visible light-active photocatalysts, J. Mater. Chem. 22(17) (2012) 8345 - 8353.

[10] W. Dong, C. Zhu, Use of ethylene oxide in the sol-gel synthesis of α-Fe_2O_3 nanoparticles from Fe (III) salts, J. Mater. Chem. 12(6) (2002) 1676 - 1683.

[11] C. S. Chen, T. G. Liu, X. H. Chen, L. W. Lin, Q. C. Liu, Q. Xia, Z. W. Ning, Preparation and magnetic property of multi-walled carbon nanotube/α-Fe_2O_3 composites, Trans. Nonferrous Met. Soc. China 19(6) (2009) 1567 - 1571.

[12] S. Biswas, S. Ram, Morphology and stability in a half-metallic ferromagnetic CrO_2 compound of nanoparticles synthesized via a polymer precursor, Chem. Phys. 306(1-3) (2004) 163 - 169.

[13] X. H. Jia, H. J. Song, Facile synthesis of monodispersed α-Fe_2O_3 microspheres through template-free hydrothermal route, J. Nanopart. Res. 14(1) (2012) 663 - 670.

[14] T. P. Ramling, A. J. A. Winnubst, C. M. van Kats, A. P. Philipse, The synthesis and magnetic properties of nanosized hematite (α-Fe_2O_3) particles, J. Colloid Interface Sci. 249(2) (2002) 346 - 350.